Buckling of Force-Excited Liquid-Filled Shells[1]

R. A. Uras
Reactor Engineering Division,
Argonne National Laboratory,
Argonne, IL 60439
Assoc. Mem. ASME

W. K. Liu
Department of Mechanical Engineering,
Northwestern University,
Evanston, IL 60208
Fellow ASME

The matrix equation of motion for liquid-filled shells with a particular reference to the influence of ground excitation are derived through a Galerkin/finite element discretization procedure. The modal coupling among the various combinations of axial and circumferential modes are identified. The equations for the dynamic buckling analysis of liquid-filled shells are presented. The buckling criteria of liquid-filled shells subjected to horizontal ground excitation are established. A comparison to available experimental results gives strikingly good agreement. The importance of modal interaction in the axial as well as circumferential directions is also demonstrated. This provides guidelines for a better understanding of dynamic buckling of liquid-filled shells.

1 Introduction

The complex nature of the damage recorded in recent earthquakes has indicated important gaps in our understanding of the mechanisms involved in damage and failure of liquid-filled systems. It is yet to be explained if this damage is due to simply horizontal, vertical and rocking ground motions, or whether it requires a consideration of nonlinear fluid-structure interaction, or phenomena such as lift-off.

The buckling tests by Shih and Babcock (1987) showed that buckling is predominantly influenced by the stresses resulting from the lowest response mode and the higher order shell modes play only a secondary role. However, shaking table experiments with aluminum tank models conducted by Clough and Niwa (1979) indicated that $\cos(n\theta)$-type modes were significantly excited by earthquake-type motions, possibly due to the initial imperfections of the tank geometry. Similar out-of-round modes have also been observed in the vibration tests of the full-scale thin shell water tanks conducted by Housner and Haroun (1979).

The intriguing task of identifying the loading mechanism onto an anchored liquid storage tank has been taken up by a small number of researchers. The possibility of buckling can be attributed to periodic axial membrane stresses caused by vertical seismic excitation. In the dynamic buckling analysis by Kana and Craig (1968), an uncoupled set of Mathieu's equations were obtained from the fluid-structure governing equations and only hoop stresses were considered in the stability analysis. Whereas, in the Chiba and Tani (1987) analysis, a set of coupled Mathieu's equations in the axial direction is obtained since the effect of axial modal coupling and all components of the membrane stresses are included.

Static buckling analyses due to moments caused by high lateral pressures exerted by the fluid onto the upper part of the tank revealed a possibility of buckling. This buckling mechanism has been studied by Liu and Lam (1983), Liu and Lam (1989) and Rammerstorfer et al. (1988).

A buckling analysis which considers dynamic fluid-structure interaction and modal coupling in both axial and circumferential directions is needed in order to shed light into the understanding of the damage mechanisms of anchored liquid-filled tanks due to seismic excitations. Although there has been an experimental study on the dynamic buckling characteristics of liquid-filled shells under horizontal excitation conducted by Chiba et al. (1986), little theoretical analysis of the dynamic buckling of liquid-filled shells under general seismic loading has been found in the literature.

This study introduces a method of analysis for the dynamic stability of liquid-filled shells. The discrete fluid-structure interaction equations are obtained through the use of a Galerkin/finite element procedure. An appropriate form of the membrane forces to represent the response of liquid-filled shells to seismic excitation is proposed. The conditions of buckling are established for a liquid-filled shell under horizontal ground motion. Finally, a comparison of experimental findings by Chiba et al. (1986) with the theoretical analysis is given. The present analysis yields the same buckling frequencies due to the (n)th and $(n+1)$th circumferential modal coupling as found in the experiments. It is also found that each of the experimental instability regions consists of many regions due to various axial and circumferential modal coupling. These bifurcation solutions can be identified from the present analysis.

In the next Section, a variational formulation is introduced for fluid-structure interaction problems, and the matrix governing equations for a thin cylindrical shell are obtained through a Galerkin/finite element discretization. Modal coupling for the resulting matrix equations is studied in Section 3. The dynamic stability equations are derived in Section 4. In Section 5, the experimental results of the dynamic buckling of liquid-

[1]This research has been supported by National Science Foundation Grant No. CES-8614957.

Contributed by the Pressure Vessels and Piping Division and presented at the Pressure Vessels and Piping Conference, Honolulu, Hawaii, July 23-27, 1989, of THE AMERICAN SOCIETY OF MECHANICAL ENGINEERS. Manuscript received by the PVP Division, June 10, 1990; revised manuscript received December 14, 1990.

Downloaded From: https://pressurevesseltech.asmedigitalcollection.asme.org on 06/28/2019 Terms of Use: http://www.asme.org/about-asme/terms-of-use
Copyright © 1991 by ASME

filled shells by Chiba et al. (1986) are compared with the present study and the findings are summarized in Section 5. Finally, Section 6 is devoted to answer some key questions on buckling failure of anchored tanks.

2 Formulation of Fluid-Structure Interaction

The principle of virtual work statement for a structure subjected to hydrodynamic loads due to an inviscid, incompressible fluid can be expressed as

$$\int_\Omega \delta u_{i,j}\tau_{ij}d\Omega + \int_\Omega \rho\delta u_i\ddot{u}_i d\Omega - \int_\Gamma \delta u_i P_d(\ddot{\mathbf{u}}, \mathbf{x})n_i d\Gamma - \int_\Gamma \delta u_i P_F(\mathbf{x}, t)n_i d\Gamma - \int_\Gamma \delta u_i P_L(\mathbf{x})n_i d\Gamma = 0 \quad (1)$$

where Γ, n_i, x_i and u_i denote the fluid-structure interface boundary, the outward normal to the structural surface, the spatial coordinates, and the structural displacement components, respectively. Ω is the domain of the structure; τ_{ij} is the Cauchy stress tensor; ρ is the structural mass density. P_d, P_F and P_L are the fluid-structural vibrational pressure, the pressure due to ground motion, and hydrostatic fluid pressure, respectively, (Liu and Uras, 1989). The spatial derivatives are denoted by a subscripted "," and repeated indices indicate sum. A superposed dot designates the temporal derivative.

After expanding τ_{ij}, u_i, P_d, P_F, and n_i into the zeroth and first-order parts via a consistent linearization procedure and rearranging terms, the zeroth and first-order equations are identified.

Zeroth Order

$$\int_\Omega \rho\delta u_i\ddot{u}_i d\Omega - \int_\Gamma \delta u_i m^{\text{ad}}(\mathbf{x}, t)n_i d\Gamma + \int_\Omega \delta u_{i,j}\tau_{ij}d\Omega = \int_\Gamma \delta u_i P_F(\mathbf{x}, t)n_i d\Gamma + \int_\Gamma \delta u_i P_L(\mathbf{x})n_i d\Gamma \quad (2)$$

First Order

$$\int_\Omega \rho\delta u_i\Delta\ddot{u}_i d\Omega - \int_\Gamma \delta u_i\Delta m^{\text{ad}}(\mathbf{x}, t)n_i d\Gamma + \int_\Omega \delta u_{i,j}C^t_{ijkm}\Delta u_{k,m}d\Omega + \int_\Omega \delta u_{i,j}\tau^0_{j1}\Delta u_{i,1}d\Omega = 0 \quad (3)$$

where C^t_{ijkm}, τ^0_{j1} and δ_{ik} are the material response tensor, the time-dependent Cauchy stress tensor arising from Eq. (2), and the Kronecker delta, respectively. In expanding the material response part of the incremental Cauchy stress tensor a Truesdell rate is employed. The added fluid inertia and the surface normal are defined as

$$m^{\text{ad}}(\mathbf{x}, t) \overset{\text{def}}{=} \frac{\partial P_d(\ddot{\mathbf{u}}, x, t)}{\partial\ddot{u}_j}\ddot{u}_j \quad (4a)$$

$$\Delta m^{\text{ad}}(\mathbf{x}, t) \overset{\text{def}}{=} \frac{\partial P_d(\ddot{\mathbf{u}}, \mathbf{x}, t)}{\partial\ddot{u}_j}\Delta\ddot{u}_j \quad (4b)$$

and

$$\Delta n_i \overset{\text{def}}{=} \Delta u_{k,k}n_i - \Delta u_{m,i}n_m \quad (4c)$$

respectively.

The following guidelines together with the assumptions of the classical shell theory are adopted to obtain the discretized equations of motion:

- the rotational inertia which is assumed of higher order is neglected;
- the standard reduction procedure commonly employed in plane stress problems is applied to the constitutive relation for linear elastic materials;
- the initial state of stress is assumed to be governed by the membrane stresses; therefore, the higher order curvature terms are neglected;
- since small deformation theory is used, total fluid pressure acting upon the shell wall and its derivatives are computed at the initial state of stress;
- Galerkin method is applied to discretize the governing equations; the three displacement components are decomposed into I axial and N circumferential modal components:

$$u(z,\theta,t) = \sum_{i=1}^{I}\sum_{n=0}^{N} u_{in}(t)\Psi_i(z)\cos n\theta \quad \text{(axial)} \quad (5a)$$

$$v(z,\theta,t) = \sum_{i=1}^{I}\sum_{n=0}^{N} v_{in}(t)\phi_i(z)\sin n\theta \quad \text{(circumferential)} \quad (5b)$$

$$w(z,\theta,t) = \sum_{i=1}^{I}\sum_{n=0}^{N} w_{in}(t)\phi_i(z)\cos n\theta \quad \text{(radial)} \quad (5c)$$

The axial mode shapes are taken as

$$\phi_i(z) = A_{1i}\cosh\lambda_i z + A_{2i}\cos\lambda_i z + A_{3i}\sinh\lambda_i z + A_{4i}\sin\lambda_i z \quad (6a)$$

and

$$\Psi_i(z) = A_{1i}\sinh\lambda_i z - A_{2i}\sin\lambda_i z + A_{3i}\cosh\lambda_i z + A_{4i}\cos\lambda_i z \quad (6b)$$

where

$$A_{1i} = -A_{2i} = 1 \quad A_{3i} = -A_{4i} = -\frac{\cosh\lambda_i L + \cos\lambda_i L}{\sinh\lambda_i L + \sin\lambda_i L}$$

and $\lambda_i L$ are the roots of

$$\cosh\lambda_i L\cos\lambda_i L = -1$$

After applying the Galerkin discretization to the variational equation, Eq. (3), the global matrix equation which governs the dynamic stability is obtained

$$\mathbf{M}\ddot{\mathbf{d}} + \mathbf{K}\mathbf{d} + \mathbf{K}^*(t)\mathbf{d} = 0 \quad (7)$$

where $\mathbf{M}$, $\mathbf{K}$, $\mathbf{K}^*(t)$ and $\mathbf{d}$ are the general mass (including the fluid added mass) matrix, the stiffness matrix, the time-dependent geometrical stiffness matrix, and the generalized displacement vector, respectively.

3 Governing Equations for the Dynamic Stability Analysis of Liquid-Filled Shells

The effect of the geometric stiffness and load correction matrices is incorporated in the time-dependent coefficient matrix $\mathbf{K}^*(t)$. Physical systems modeled through equations of this type are referred to as parametrically excited systems.

For stability analysis, an orthogonality transformation is applied to Eq. (7)

$$(\mathbf{d})_n = (\mathbf{Q})_n(\mathbf{u})_n \quad \text{no sum on } n \quad (8)$$

where $(\mathbf{Q})_n$ are the diagonal entries of the orthogonal matrix $\mathbf{Q}$

$$\mathbf{Q} = \begin{bmatrix} (\mathbf{Q})_1 & 0 & 0 & 0 & 0 & 0 \\ 0 & (\mathbf{Q})_2 & 0 & 0 & 0 & 0 \\ 0 & 0 & \cdot & 0 & 0 & 0 \\ 0 & 0 & 0 & (\mathbf{Q})_n & 0 & 0 \\ 0 & 0 & 0 & 0 & \cdot & 0 \\ 0 & 0 & 0 & 0 & 0 & (\mathbf{Q})_N \end{bmatrix} \quad (9)$$

By applying this transformation, the total mass matrix is normalized to the identity matrix and the stiffness matrix is reduced to a diagonal matrix, $\mathbf{\Lambda}$, of natural frequencies, ω^2_{in}, for $i = 1$ through I and $n = 1$ through N. Consequently, Eq. (7) becomes

$$\ddot{\mathbf{u}} + [\mathbf{\Lambda} + \mathbf{G}(t)]\mathbf{u} = \mathbf{0} \quad (10)$$

where

Downloaded From: https://pressurevesseltech.asmedigitalcollection.asme.org on 06/28/2019 Terms of Use: http://www.asme.org/about-asme/terms-of-use

$$\Lambda = \begin{bmatrix} (\Lambda)_{11} & 0 & 0 & 0 & 0 & 0 \\ 0 & (\Lambda)_{22} & 0 & 0 & 0 & 0 \\ 0 & 0 & \cdot & 0 & 0 & 0 \\ 0 & 0 & 0 & (\Lambda)_{nn} & 0 & 0 \\ 0 & 0 & 0 & 0 & \cdot & 0 \\ 0 & 0 & 0 & 0 & 0 & (\Lambda)_{NN} \end{bmatrix} \tag{11}$$

$$\mathbf{G}(t) = \begin{bmatrix} (\mathbf{G}^0)_{11} & (\mathbf{G}^1)_{12} & 0 & 0 & 0 & 0 \\ (\mathbf{G}^{(-1)})_{21} & (\mathbf{G}^0)_{22} & (\mathbf{G}^1)_{23} & 0 & 0 & 0 \\ 0 & \cdot & \cdot & \cdot & 0 & 0 \\ 0 & 0 & (\mathbf{G}^{(-1)})_{n,n-1} & (\mathbf{G}^0)_{nn} & (\mathbf{G}^1)_{n,n+1} & 0 \\ 0 & 0 & 0 & \cdot & \cdot & \cdot \\ 0 & 0 & 0 & 0 & (\mathbf{G}^{(-1)})_{N,N-1} & (\mathbf{G}^0)_{NN} \end{bmatrix} \tag{12}$$

and

$$\mathbf{u} = [(\mathbf{u})_1, (\mathbf{u})_2, \ldots, (\mathbf{u})_n, \ldots, (\mathbf{u})_N]^T \tag{13}$$

The submatrices in Eqs. (11) and (12) are defined as:

Eigenvalue submatrices

$$(\mathbf{Q})_n^T(\mathbf{K})_{nn}(\mathbf{Q})_n = (\Lambda)_{nn} \quad \text{no sum on } n \tag{14}$$

Geometric stiffness submatrices due to vertical ground excitation

$$(\mathbf{Q})_n^T(\mathbf{K}^{*0})_{nn}(\mathbf{Q})_n = (\mathbf{G}^0)_{nn} \quad \text{no sum on } n \tag{15}$$

Geometric stiffness submatrices due to horizontal ground excitation

$$(\mathbf{Q})_n^T(\mathbf{K}^{*1})_{n,n+1}(\mathbf{Q})_{n+1} = (\mathbf{G}^1)_{n,n+1} \quad \text{no sum on } n \tag{16}$$

$$(\mathbf{Q})_n^T(\mathbf{K}^{*(-1)})_{n,n-1}(\mathbf{Q})_{n-1} = (\mathbf{G}^{(-1)})_{n,n-1} \quad \text{no sum on } n \tag{17}$$

Therefore, Λ and $\mathbf{G}(t)$ are $N \times N$ matrices and each submatrix is $(3I) \times (3I)$. The block-diagonal terms in $\mathbf{G}(t)$ reflect the effect of vertical ground excitation, whereas the nonzero block-off-diagonal terms arise as a result of horizontal ground excitation and rocking motion.

Since the membrane theory yields a good approximation for the actual stress distribution away from the built-in end, the membrane stresses can be assumed of the following form:

$$N_z^0(z,\theta,t) = N^z(t)\Gamma_z(z)[a_z + b_z\cos\theta] \tag{18a}$$

$$N_\theta^0(z,\theta,t) = N^\theta(t)\Gamma_\theta(z)[a_\theta + b_\theta\cos\theta] \tag{18b}$$

$$N_{z\theta}^0(z,\theta,t) = N^{z\theta}(t)\Gamma_{z\theta}(z)\ b_{z\theta}\sin\theta \tag{18c}$$

where $N^\alpha(t)$ are the time-dependent membrane force amplitudes; $\Gamma_\alpha(z)$ represent the axial distribution of membrane forces; a_α and b_α account for the relative weights of vertical and horizontal ground excitations, respectively; and $\alpha = z$ or θ or $z\theta$.

The membrane force amplitudes can be obtained by expanding $N^\alpha(t)$ into Fourier series

$$N^\alpha(t) = \sum_{s=1}^{S} [N_{1s}^\alpha \cos(s\omega t) + N_{2s}^\alpha \sin(s\omega t)] \quad \alpha = z \text{ or } \theta \text{ or } z\theta \tag{19}$$

where S is the truncation limit for the expansion. N_{1s}^α and N_{2s}^α are the Fourier coefficients for the cosine and sine series, respectively.

For stability analysis, three nondimensional parameters ϵ_z, ϵ_θ and $\epsilon_{z\theta}$ are defined for the axial, circumferential and torsional stresses, respectively,

$$\epsilon_z = \frac{N_{11}^z}{N_{\text{cr}}^z}; \quad N_{\text{cr}}^z = \frac{Eh^2}{R\sqrt{3(1-\nu^2)}} \tag{20}$$

$$\epsilon_\theta = \frac{N_{11}^\theta}{N_{\text{cr}}^\theta}; \quad N_{\text{cr}}^\theta = 0.927\left(\frac{h}{R}\right)^{5/2}\left(\frac{R}{L}\right)(hE) \tag{21}$$

$$\epsilon_{z\theta} = \frac{N_{11}^{z\theta}}{N_{\text{cr}}^{z\theta}}; \quad N_{\text{cr}}^{z\theta} = 0.755\left(\frac{h}{R}\right)^{5/4}\left(\frac{R}{L}\right)^{1/2}(hE) \tag{22}$$

where E, ν, h, and R the Young modulus, the Poisson ratio, the shell thickness, and the radius of the shell, respectively, and the subscript cr refers to the respective static critical buckling forces (Yamaki (1984)).

The Fourier expansion of the time-dependent geometric stiffness matrix becomes

$$\mathbf{G}(t) = \sum_{s=1}^{S} [\mathbf{G}_1^s \cos(s\omega t) + \mathbf{G}_2^s \sin(s\omega t)] \tag{23}$$

where $\mathbf{G}_1^s$ and $\mathbf{G}_2^s$ are the Fourier coefficients.

In summary, the governing equation of motion, Eq. (10) takes the following form:

$$\ddot{\mathbf{u}} + \mathbf{C}\dot{\mathbf{u}} + \Lambda\mathbf{u} + \sum_{s=1}^{S} [\mathbf{G}_1^s \cos(s\omega t) + \mathbf{G}_2^s \sin(s\omega t)]\mathbf{u} = \mathbf{0} \tag{24}$$

where $\mathbf{C}$, a diagonal damping matrix, has been included for the completeness of the stability analysis. The ith and nth components of the $\mathbf{C}$ matrix are given by

$$c_{in} = 2\zeta_{in}\omega_{in} \tag{25}$$

where ζ_{in} is the damping coefficient associated with eigenfrequency ω_{in}.

This form of equations is commonly referred to as the coupled Hill's equation.

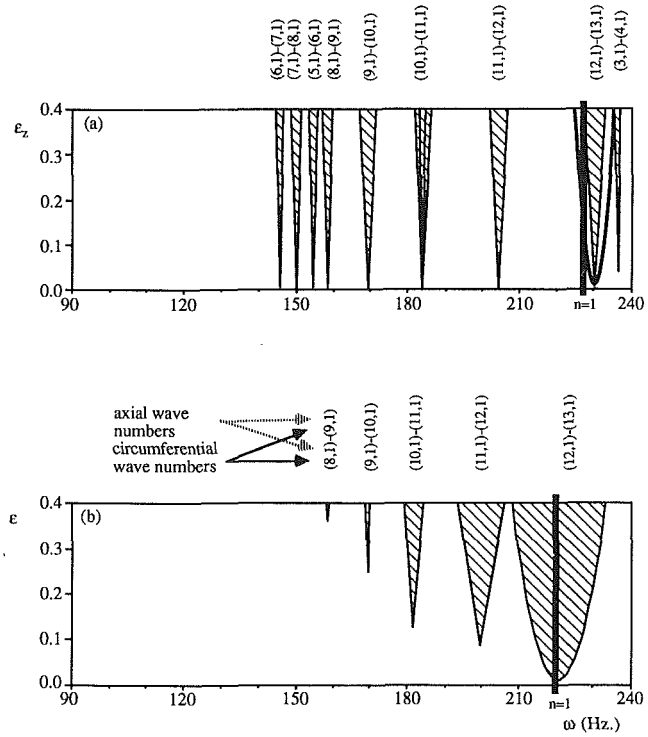

Fig. 1 Stability charts prepared using (*a*) the analysis by Liu and Uras (1989b); (*b*) the experiments by Chiba et al. (1986)

Downloaded From: https://pressurevesseltech.asmedigitalcollection.asme.org on 06/28/2019 Terms of Use: http://www.asme.org/about-asme/terms-of-use

4 Dynamic Buckling Analysis

In seismic analysis, the response of the fluid-structure system is dominated by only a few modes. With this assumption, Eq. (24) can be simplified to

$$\ddot{\mathbf{u}} + \mathbf{C}\dot{\mathbf{u}} + \Lambda\mathbf{u} + \epsilon\mathbf{G}\mathbf{u}\cos\omega t = \mathbf{0} \tag{26}$$

where ω and ϵ represent a typical dominant frequency and the normalized amplitude of the seismic excitation, respectively. A superposed dot denotes time differentiation; and $\mathbf{u}$ is the vector of modal displacement amplitudes. When mass proportional damping is adopted, the ith and nth components of the damping matrix, $\mathbf{C}$, are given by

$$c_{in} = 2\zeta_{\min}\frac{\omega_{in}^2}{\omega_{\min}} \quad \text{for } i = 1, \ldots, I \text{ and } n = 1, \ldots, N \tag{27}$$

where I and N are the total number of modes in the axial and circumferential directions, respectively; $\omega_{\min}$ and $\zeta_{\min}$ are the lowest frequency and the corresponding damping coefficient, respectively. Λ is a diagonal matrix of natural frequencies, ω_{in}^2. G is the block-tri-diagonal matrix

$$\mathbf{G} = \begin{bmatrix} (\mathbf{G})_{11} & (\mathbf{G})_{12} & 0 & 0 & 0 & 0 & 0 \\ (\mathbf{G})_{21} & (\mathbf{G})_{22} & (\mathbf{G})_{23} & 0 & 0 & 0 & 0 \\ 0 & \cdot & \cdot & \cdot & 0 & 0 & 0 \\ 0 & 0 & (\mathbf{G})_{n,n-1} & (\mathbf{G})_{nn} & (\mathbf{G})_{n,n+1} & 0 & 0 \\ 0 & 0 & 0 & (\mathbf{G})_{n+1,n} & \cdot & \cdot & 0 \\ 0 & 0 & 0 & 0 & \cdot & \cdot & (\mathbf{G})_{N-1,N} \\ 0 & 0 & 0 & 0 & 0 & (\mathbf{G})_{N,N-1} & (\mathbf{G})_{NN} \end{bmatrix} \tag{28}$$

The diagonal blocks of Eq. (28) vanish if only horizontal ground excitation is applied to the fluid-structure system, which is the focus in this study. Equation (26) falls into the category of coupled Hill's equations. General buckling solutions for this equation are introduced by Uras and Liu (1989).

The location of an instability region on a stability chart is fixed by the natural frequencies of the respective modes. The size of an instability region, is a measure of vulnerability to buckling and depends on the system eigenmodes.

5 Results and Discussion

In this section, a comparison of results obtained by the present method of analysis and Chiba et al.'s (1986) experiments is given for a liquid-filled shell with the following data:

R	(radius)	0.1 m
h	(thickness)	0.0025 R
L	(length)	1.607 R
E	(Young's modulus)	5.56 GPa
ν	(Poisson's ratio)	0.3
ρ	(shell mass density)	$1.405 \cdot 10^3$ kg/m^3
ρ_F	(fluid mass density)	$1.0 \cdot 10^3$ kg/m^3

The experimental and theoretical values of the first $\cos\theta$-mode are 220 Hz and 227 Hz, respectively. The comparison of results to the Chiba et al. (1986) experiments are depicted in Figs. 1(a) and (b). Major buckling modes around this mode are identified as $\cos 12\theta$ and $\cos 13\theta$. A second circumferential modal coupling is found to be between $\cos 3\theta$ and $\cos 4\theta$ for the first axial mode. The buckling mode shape (as indicated by the thick curve in Fig. 1(a) obtained from the present analysis agree with the region obtained by Chiba et al. as shown in Fig. 1(b). However, in the experiments, only the axial mode (1,1) and the circumferential mode (12,13) could be identified although the second region is within ±5 percent of the first $\cos\theta$-mode. It should be noted that only five buckling frequencies in the vicinity of the $\cos\theta$-mode are available for comparison.

In summary, the general characteristics of the theoretical results for the liquid-filled shell can be summarized as follows (refer to Figs. 1(a) and (b):

(i) All the locations of the main buckling frequencies due to (n)th and (n + 1)th circumferential modal coupling predicted by the analysis correspond to those of the experiments.

(ii) Around the $\cos\theta$-frequency, a large number of buckling frequencies are clustered together, which are depicted as one instability region on the experimental stability charts (these regions are indicated by thick curves in Figs. 1(a) and (b)).

(iii) The frequency band is centered by the main buckling frequency from type (1), and includes other modes with axial and circumferential modal coupling.

For a liquid-filled geometrically perfect cylindrical shell subjected to horizontal ground excitation, only one type of instability region is expected when the fluid-structure system is subjected to horizontal ground motion

$$\omega \approx \omega_{in} + \omega_{j,n+1} \tag{29}$$

On the other hand, in the experimental spectra given by Chiba et al. (1986) buckling frequencies of the following types are found:

1 The majority of the buckling frequencies are due to axial modal coupling and the coupling between the (n)th and (n + 1)th circumferential modes induced by horizontal ground motion (compare with Eq. (29))

$$\omega \approx \omega_{in} + \omega_{j,n+1} \tag{30a}$$

2 Due to the influence of vertical ground motion and/or externally applied axial forces

$$\omega \approx 2\omega_{in} \tag{30b}$$

3 Due to contribution from the nonlinearities of the specimen

(3a) $\omega \approx \omega_{in} + \omega_{im} + \omega_{i,n+m}$ (30c)

(3b) $\omega \approx \omega_{in} + \omega_{j,n+2}$ (30d)

The present analysis agrees with their experimental analysis in predicting buckling frequencies induced by the axial and circumferential modal coupling (Eq. (30a)). It seems that in Chiba et al. experiments, the $n = 0$ breathing modes, called principle buckling modes, are also excited (Eq. (30b)). One possible explanation of this occurrence, is vertical motion introduced by the shaking table and uncertainties in the experiments. The third set of instability regions (Eqs. (30c and d)) can be induced either by imperfections in the structure and/or by difficulties of identifying modes due to the coupling between axial and circumferential modes. However, the major buckling region is governed by Eq. (29), and the rest is of minor importance.

6 Conclusions

The aim of this paper is to search for a fundamental understanding of the various possible failure mechanisms of anchored storage tanks under seismic excitation.

The fluid-structure interaction problem is formulated by a variational statement. A Galerkin/finite element discretization is applied to obtain the governing matrix equations. For a better understanding of the transient failure mechanisms, the shell membrane forces are decomposed into a hydrostatic part,

Downloaded From: https://pressurevesseltech.asmedigitalcollection.asme.org on 06/28/2019 Terms of Use: http://www.asme.org/about-asme/terms-of-use

and into a dynamic part due to various components of the ground motion. The modal coupling in the axial and circumferential directions due to different types of seismic loads is identified. The significance of the axial and circumferential cross-coupling in the failure of tanks is also revealed. For dynamic stability analysis, the matrix equations are cast into a set of coupled Hill's equations by employing an orthogonality transformation. A comparison of the results obtained through the present study, and the available experimental findings reveals very good agreement in predicting instability conditions.

The significant buckling phenomena for failure conditions in which the buckling modes are not exactly known from the shaking table experiments can be identified from the conditions established in the present analysis.

References

Chiba, M., and Tani, J., 1987, "Dynamic Stability of Liquid-Filled Cylindrical Shells Under Vertical Excitation, Part II: Theoretical Results," *Earthquake Engineering and Structural Dynamics*, Vol. 15, pp. 37–51.

Clough, D. P., and Niwa, A., 1979, "Static Tilt Tests of a Tall Cylindrical Liquid Storage Tank," University of California Earthquake Engineering Research Center, Report No. UCB/EERG 79-06, Feb.

Housner, G. W., and Haroun, M. A., 1979, "Vibration Tests of Full-Scale Liquid Storage Tanks," *Proceedings of 2nd U.S. International Conference on Earthquake Engineering*, Stanford University, August.

Kana, D. D., and Craig, R. R., Jr., 1968, "Parametric Oscillations of a Longitudinally Excited Cylindrical Shell Containing Liquid," *Journal of Spacecraft*, Vol. 5, pp. 13–21.

Liu, W. K., and Lam, D., 1983, "Nonlinear Analysis of Liquid-Filled Tank," *Journal of Engineering Mechanics*, Vol. 109, pp. 1344–1357.

Liu, W. K., and Lam, D., 1989, "Numerical Analysis of Diamond Buckles," *Finite Elements in Analysis and Design*, Vol. 4, pp. 291–302.

Liu, W. K., and Uras, R. A., 1989, "Transient Failure Analysis of Liquid-Filled Shells," *Nuclear Engineering and Design*, Vol. 117, pp. 107–157.

Rammerstorfer, F. G., Scharf, K., Fischer, F. D., and Seeber, R., 1988, "Collapse of Earthquake Excited Tanks," *Res Mechanica*, Vol. 25, pp. 129–143.

Shih, C. F., and Babcock, C. D., 1987, "Buckling of Oil Storage Tanks in SPPL Tank Farm During the 1979 Imperial Valley Earthquake," ASME JOURNAL OF PRESSURE VESSEL TECHNOLOGY, Vol. 109, pp. 249–255.

Uras, R. A., and Liu, W. K., 1989, "Dynamic Stability Characteristics of Liquid-Filled Shells," *Earthquake Engineering and Structural Dynamics Journal*, Vol. 18, pp. 1219–1231.

Yamaki, N., 1984, *Elastic Stability of Circular Cylindrical Shells*, North-Holland, Amsterdam.

Downloaded From: https://pressurevesseltech.asmedigitalcollection.asme.org on 06/28/2019 Terms of Use: http://www.asme.org/about-asme/terms-of-use